

Article

Defense and Protection of the Marine Coastal Areas and Human Health: A Case Study of Asbestos Cement Contamination (Italy)

Roberta Somma ^{1,*} , Salvatore Giacobbe ², Francesco Paolo La Monica ³, Maria Letizia Molino ⁴, Marina Morabito ² , Sebastiano Ettore Spoto ¹ , Salvatore Zaccaro ⁵ and Giuseppe Zaffino ³

¹ Department of Mathematical and Computer Sciences, Physical Sciences and Earth Sciences, University of Messina, Viale F. Stagno d'Alcontres, 31, Sant'Agata, 98166 Messina, Italy

² Department of Chemical, Biological, Pharmaceutical and Environmental Sciences, University of Messina, Viale F. Stagno d'Alcontres, 31, Sant'Agata, 98166 Messina, Italy; salvatore.giacobbe@unime.it (S.G.); marina.morabito@unime.it (M.M.)

³ Ambiente Lab, Granatari, 4, 98164 Messina, Italy; gzaffino@me.com (F.P.L.M.); gzaffino@icloud.com (G.Z.)

⁴ Metropolitan City of Messina, Palazzo dei Leoni, Corso Cavour, 98122 Messina, Italy

⁵ pH3 Engineering S.r.l., Via Caio Duilio, 2, 98123 Messina, Italy; szaccaro@ph3srl.it

* Correspondence: rsomma@unime.it

Abstract: Pivotal environmental geology research was carried out in the protected area of Cape Peloro (Messina, NE Sicily, Italy). The main aims were the ascertainment of the presence of Asbestos Cement Materials (ACMs), their mapping, and, consequently, an estimation of the potential risk for human health and marine coastal environments. The beaches surveyed covered 4500 m of coastline. Through high-resolution photographic surveys, over 520 fiber cement fragments were documented on the beaches as well as in beach deposits. The materials, after microscope, SEM-EDS, and FTIR analyses, were found to be composed of Portland cement with chrysotile and crocidolite fibers. Fragments of ACMs showed typical corrugated forms with centimeter-to-decimeter sizes and prevailing well-rounded, platy, and sub-elongate shapes. In a few localities, some fragments were found to be angular or friable. Furthermore, some fragments found on the beach were covered by conspicuous encrustations of marine organisms, testifying to their long staying in shallow-water marine environments. Illicit landfills and abandoned materials were identified in natural sections on the coastal plain. Most of the rounded ACMs were characterized by their surface texture, with mm-size asbestos fibers exposed on the surface due to significant weathering and abrasion. Notably, new fragments appeared after storms. Significant criticisms have been made related to the ACMs, analogously to what was reported for other Italian marine beaches. Possible intervention and reclamation activities cannot limit themselves to removing the fragments on the beach, as fragments are immersed in the coastal sediments at different depths and are also found in the marine deposits. Here, it is underlined that any asbestos removal and reclamation activities, if not designed and based on a multidisciplinary approach and knowledge of local coastal dynamics and the meteo-marine climate, will be very expensive and ineffective.

Keywords: marine coasts; protected areas; defense and conservation; asbestos cement materials; wastes; contamination; human health risk; medical geology



Citation: Somma, R.; Giacobbe, S.; La Monica, F.P.; Molino, M.L.; Morabito, M.; Spoto, S.E.; Zaccaro, S.; Zaffino, G. Defense and Protection of the Marine Coastal Areas and Human Health: A Case Study of Asbestos Cement Contamination (Italy). *Geosciences* **2024**, *14*, 98. <https://doi.org/10.3390/geosciences14040098>

Academic Editors: Angelos G. Maravelis and Jesus Martinez-Frias

Received: 18 February 2024

Revised: 26 March 2024

Accepted: 28 March 2024

Published: 1 April 2024



Copyright: © 2024 by the authors. Licensee MDPI, Basel, Switzerland. This article is an open access article distributed under the terms and conditions of the Creative Commons Attribution (CC BY) license (<https://creativecommons.org/licenses/by/4.0/>).

1. Introduction

The general term “asbestos” is commonly used to refer to six silicate minerals belonging to the groups of serpentine (chrysotile) and amphiboles (amosite, actinolite, anthophyllite, crocidolite, and tremolite) [1].

Their peculiar chemical–physical properties (fireproof, lightweight, high tensile strength, electrical resistance, durability, and flexibility) have been exploited by industries since the early–mid-19th century to produce fiber cements, insulation, and textile materials [2]. Their diffusion in military, industrial, agricultural, and residential structures was due to

their low cost and significant physical properties. The asbestos cement materials (ACMs) were denoted as Eternit (a registered trademark) by a famous industry due to their long life. Asbestos minerals were dug out from quarries worldwide (Canada, USA, South Africa, Russia, and Italy). In the Italian Alps, at Balangero (Turin), was one of the largest industrial-scale mines in Europe [3].

Asbestos cement is a lightweight, light grey product (specific weight: 1.8–2.2 g/cm³) composed of a homogenous matrix of cement (Portland cement, CaCO₃) mixed with a reinforcing grid of asbestos fibers, which are present in percentages ranging from 10 to 15% by weight. Quartz sands and artificial glass wool may also be added to the mixture. Although the grid of asbestos fibers is embedded in the ACM cement matrix and immobilized, when the matrix degrades, because of long-term weathering, abrasion, and erosion, asbestos fibers are inevitably released into the atmosphere, hydrosphere, and lithosphere, contaminating natural resources. The most widespread asbestos minerals that are mixed in the fiber cement produced in southern Italy are chrysotile and crocidolite, which occur in mossy aggregates in fibrous and asbestiform habitats. Indeed, these minerals are easily crumbled into smaller bundles of fibrils. Chrysotile belongs to the serpentine subgroup of phyllosilicates [Mg₃ Si₂O₅(OH)₄] [4] and has a white color (it is also known as white asbestos). Crocidolite is a variety of riebeckite (also known as blue asbestos) [Na₂(Fe²⁺₃ Fe³⁺₂)Si₈O₂₂(OH)₂] [4] characterized by a typical cobalt dark blue to lavender color, which exhibits waved fibers [5]. Regarding their behavior, chrysotile has a lower tensile strength and higher heat resistance than crocidolite [5]. Due to their different colors, aspects, and size, these two fiber minerals can be easily recognized in the ACMs present in the territory via the naked eye or a 10× magnifying lens.

The most widespread asbestos cement products were corrugated roofings, which is mostly still present (and, in part, protected by special encapsulating paints), water tanks, and tubes. The Eternit sheets used in the corrugated surfaces were about 1 m wide, from 1.2 to 3.75 m long, and had thicknesses ranging from 4 to 20 mm. The number of undulations could range from 5 to 7 with a mean amplitude of 177 mm in the width of the crests. Mm-sized ornamentations, present on one side of this material to create the rough surface, were usually made up of honeycomb-like textures (with mark alignments oblique to the crests) or of aligned square marks (similar to “dome and basin like” shapes, aligned parallel and orthogonal to the crests).

ACM continued to be produced and used in Italy until the beginning of the 1990s, before law n. 257 of 1992 [6], which banned its production and use because of its toxicity and consequent high health hazard. The Italian legislation, with the ministerial decree of 1994 [7], regulated analytical instrumentation as well as removal and remediation activities. After the Italian legislative decree of 1997 [8], ACMs represented a critical issue, requiring the management of competent authorities to ensure their removal and remediation in controlled landfills. In 1999, the ban was also extended to the rest of the European Union [9].

According to the Italian legislative decree n. 152 of 2006 [10], ACMs were classified as dangerous wastes (CER code 17 06 01* 17 06 05*). Old corrugated roofings and pipes are still present in the Italian territory. Moreover, after the ACM ban, expensive taxes were levied for the disposal activities. Therefore, the illegal abandonment of these wastes in uncontrolled areas of the territory (rivers, streams, slopes, and coastal areas) increased, leading to the diffusion of these materials in Italy. This was especially common during the 1990s [11] but still occurs.

After the laws above were established, the Italian legislation further evolved, conferring the affected regions with the competences to carry out the necessary actions to protect the environment. With law n. 257 [6], the regions were entrusted with the drawing up of plans for environmental protection, as well as decontamination, disposal, and remediation activities, in order to reduce the hazards deriving from human/environment–asbestos interactions.

In particular, at the regional scale, the Sicilian regional law of 2014 [12] provided indications for the adoption of measures aimed at the prevention and environmental

remediation of pollution from asbestos fibers. The coordination of these activities and procedures was to be achieved by the regional administration, the Regional Agency for the Protection of the Environment (ARPA), the Provincial Health Company (ASP), and the local authorities. The role of the municipalities is fundamental to the protection of citizens' health and mitigation of the risks associated with exposure to asbestos. The creation of a census of sites or buildings in which ACMs are present, and the progressive removal of ACMs, represent activities to be carried out by the municipalities. According to art. 4 c.1, letter b of the regional law [12], the municipalities must have a "Municipal asbestos plan".

2. Human Health and Environmental Risks

Epidemiological studies have proved that all the above-mentioned asbestos minerals are classified as carcinogens by the International Agency for Research on Cancer (IARC) [13].

The interaction between geological materials, such as asbestos minerals, and human, animal, and plant health is an issue that is frequently analyzed by a recent discipline, medical geology [14]. There may be many possible interactions and pathways of direct or indirect exposure. The limits for the concentration of asbestos fibers in the air, water, and soil differ according to country and are based on the sources of exposure. The health effects on humans caused by professional, environmental, and secondary exposure to asbestos may appear decades later. Indeed, disease may appear a mean of 46 years after exposition, at a mean age of 70 years [15].

The most relevant sources of asbestos fibers in the air are anthropogenic [16,17], and may be due to the activities of asbestos mines near urban areas or to vehicular traffic intensities. The natural contamination of water may be dependent on the natural asbestos minerals present in the rocks, whereas the anthropogenic contamination of drinking waters may be due to the release of fibers from old asbestos-cement pipes or containers. The fracture and size (length and diameter) of the asbestos fibers [18] represent the most crucial parameters of their toxicity [19]. These features make these minerals highly carcinogenic and responsible for uncommon, dangerous diseases, including asbestosis, tumors in the lung [20,21], larynx and ovaries, mesothelioma, a rare malignancy of the serosal membranes [15], and serous covering of the testis [22]. Mesothelioma is commonly associated with prior extensive inhalation of crocidolite [23], tremolite, and amosite fibers, but other fibrous minerals (such as erionite, fluoro-edenite, and balangeroite) [24] can also be responsible for this disease. Moreover, the pathogenesis of malignant peritoneal mesothelioma (abdominal) could also be affected by asbestos fiber ingestion caused by environmental exposure, in addition to their inhalation [25].

In Italy, 31,572 cases of mesothelioma were reported in the VII report of 2021 [15]. A total of 17.4% of cases were inferred to be caused by unknown exposure. In Messina, Catania, and Palermo, the incidence of unknown exposure mesothelioma (calculated according to the number of villages) is among the highest among the Sicilian population [15]. The ACM health risk will be present for decades. Indeed, asbestos bans should lead to a decrease in the incidence of mesothelioma with an age-standardized rate of 20–40 years [26,27]. Due to the long time it takes for the effects to manifest and the uncertainty of their causes, the precaution principle should not be neglected by the public authorities regarding asbestos, to ensure that human health and environmental safety are protected.

3. Aim of the Research

Human asbestos exposure and the related health risks should be limited everywhere but especially in recreational and tourist areas. Considering their high recreational value and tourist uses, the renowned coastal areas facing the Mediterranean Sea should be healthy environments that are regularly managed and controlled to ensure their usability. Most marine beaches are continuously overrun by dangerous and not dangerous organic and/or inorganic wastes. Indeed, marine coastal areas and the seas/oceans are the final destinations for wastes after they are illegally abandoned in the soil and transported to the

marine coast by streams/rivers and the wind [28]. The man-made organic pollutants that are most present on beaches worldwide are highly carcinogenic polychlorinated biphenyls (PCB) and plastics [29]. These types of wastes, a common focus of research, are persistent and may undergo long-term transport due to their low degradation rates [29–33]. Other inorganic wastes widespread on beaches, such as glass, bricks, pottery, tiles, mortar, and cement, including ACMs, arise from building construction and demolition materials [34]. The ACMs that usually are found in soils and beaches mostly consist of entire or fragments of corrugated roofing, but remnants of planar slabs, tanks, pipes, and facade coatings are also present [29]. In such cases, the provenance of the ACMs may also be due to illegal coastal landfills and incidents that occur at sea (shipwrecks) [13,29].

In recent years, commodity and remote sensing investigations allowed Lisco et al. 2023 [29] to individuate ACMs in the beach of Marechiaro Bay at Taranto (Italy), and to prove their provenance from illegal and uncontrolled landfills created in the surrounding areas during 1980–2000. The natural consequence of this alarming research was to restrict access to the beach [29]. However, Italian scientific literature devoted to this criticism is very infrequent and most of the information on this issue is derived from the environmental associations and the media. These latter have discovered various soils and beaches contaminated by ACMs, ranging from northern to southern Italy (Friuli Venezia Giulia, Liguria, Tuscany, Lazio, Marche, Campania, Calabria, Puglia, and Sicily) [35–54].

With this in mind, inspired by the valuable research of Lisco et al. (2023) [29], a pivotal environmental geology study was carried out, starting from a protected marine coastal area of Sicily. The main aims of the present research were the ascertainment of the presence of ACMs and, in positive cases, the mapping of these ACMs in a GIS-based platform. Significant criticisms related to ACMs involving their potential risk to human health and threat to coastal environments were found regarding the Cape Peloro area (Messina, NE Sicily), indicating that it could be a suitable subject for a case study analogous to that reported for other marine beaches in Puglia.

This pivotal research, promoted by the reserve managing body (the Metropolitan City of Messina) and carried out by geologists and biologists of the University of Messina, is the first interdisciplinary approach to this alarming issue in Sicily.

4. Study Area

The study area comprises the Holocene coastal area of the Cape Peloro peninsula, extending along the whole Cape Peloro, between the localities of Canal degli Inglesi on the Tyrrhenian coast and Canal Due Torri on the Ionian coast (Figure 1a).

The study area, comprising two important lakes (the lakes of Ganzirri and Faro) and wetlands with rich fauna and flora, is a protected environmental site that falls within the Special Protection Zones (SPZs) (SPZ ITA030042—Monti Peloritani, Dorsale Curcuraci, Antennamare, and marine area of the Straits of Messina—27,993 ha, [55] partially overlapping the SPZ ITA030008—Capo Peloro—Ganzirri Lakes—60 ha [56]) and the Oriented Natural Reserve (O.N.R.) of Cape Peloro.

The SPZs, designated directly by the Member States, belong to the Natura 2000 network. The identification and delimitation of the SPZs are based entirely on scientific criteria. The network aims to protect the territories that are suitable for the conservation of sedentary and migrant birds. The lakes of Ganzirri and Faro are the largest 2 of the 38 Italian wetlands that provide Mediterranean bird flyways for many avian species [57].

Cape Peloro O.N.R. (Figure 1a), established by the Sicilian region over two decades ago, faces both the Tyrrhenian and Ionian Seas and includes two zones:

- i. Zone A (reserve), which includes the brackish water coastal lakes of Ganzirri and Faro (Figure 1), classified by the Sicilian Region as Mondial geosites due to their peculiar morphological features.
- ii. Zone B (pre-reserve), which comprises Ionian and Tyrrhenian marine beaches, four artificial canals (degli Inglesi, Faro, Due Torri, and Catuso) connecting the lakes to the sea, and one canal (Margi) connecting the lakes to each other (Figure 1).

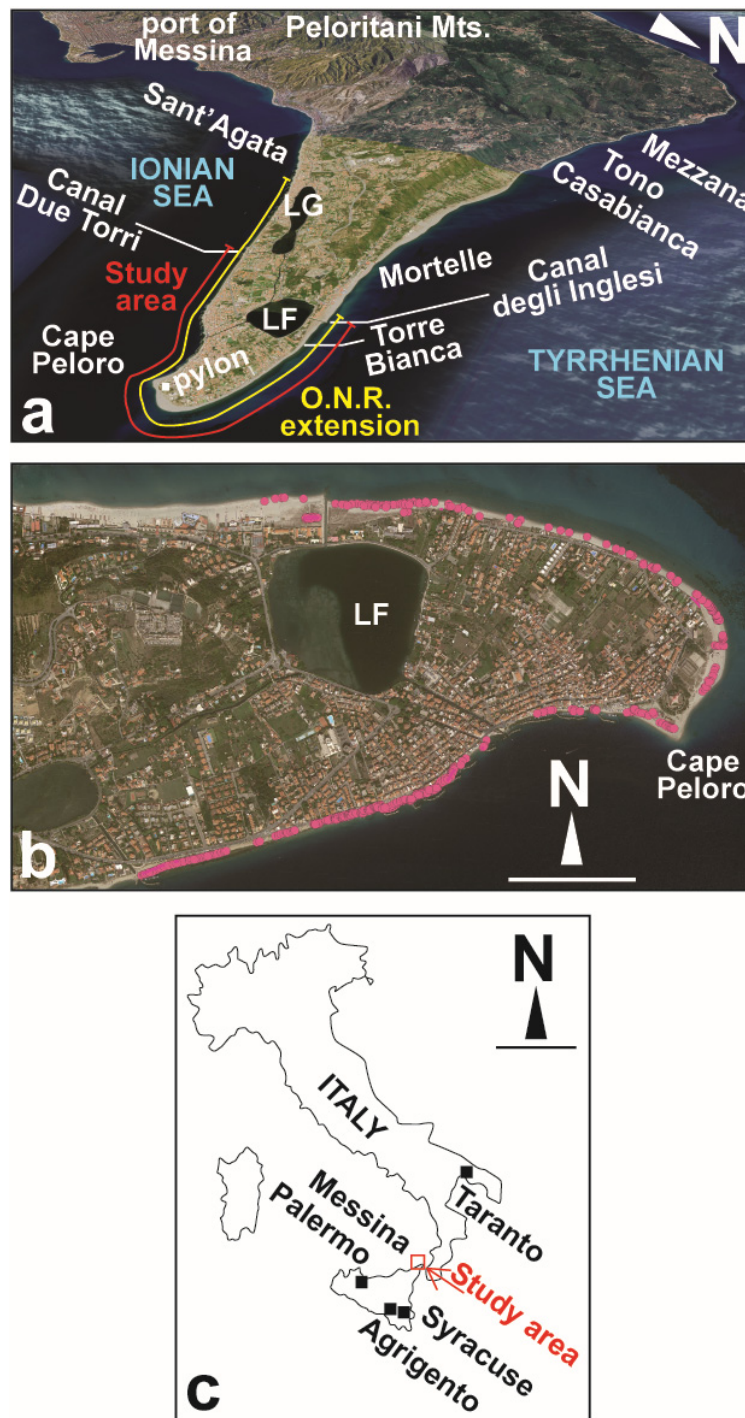


Figure 1. (a) Localization of the study area (red line) and the pre-reserve of the O.N.R. (yellow line) shown in the satellite photograph in 3D modality (Google Earth Pro). (b) GIS map of the 520 fragments of ACMs (pink circles) (QGIS 3.28.10 software). (c) The insert shows the geographic localization of the study area. The localities cited in the text are also reported. Acronyms: LF: Lake Faro, LG: Lake Ganzirri. Source: Authors.

The beaches of the study area are renowned touristic and recreational areas, hosting several beachfront resorts. The surrounding areas offer different attractions to tourists and holiday-makers, such as historical monuments, cultural foundations, scuba diving and sport centres, resorts, and several restaurants and bars. One of the most popular attractions at Cape Peloro is the “Pylon of Messina” (Figure 1), a 232 m high steel tower

that was used until 1994 to carry power lines from Calabria to Sicily. Moreover, the beauty of the landscape and the clarity of the water make Cape Peloro beach the most renowned, traditional, and heavily frequented summer location for swimming and sunbathing. Both adults and children use the free beach where, as equipment and deckchairs are lacking, direct contact with the sand is inevitable. The most impactful human activities occurring on the beach are related to fishing and the shelter and maintenance of fishing boats (especially on the Ionian side). Other human activities present in the neighboring areas are represented by the oil refinery of Milazzo (at a distance of about 35 km along the coast) and the port of Messina (at a distance of about 10 km).

The research area is stretched from the Canal degli Inglesi to the Canal Due Torri, along a belt covering about 75% of the O.N.R. marine beaches (Figure 1a). The field surveys, included natural sections, were carried out along a 4500 m long coast along the Tyrrhenian and Ionian seas during the winter of 2023–2024 (Figure 1).

The length of beach that is devoid of infrastructures and available for recreational uses varied from approximately 80 m to a few meters. Torre Bianca beach is oriented from the E–W to WNW–ESE and its width varies from approximately 80 m (to the W) to 10 m (to the E; Google Earth data, 11 July 2023 satellite photograph) (Figure 1a). Cape Peloro beach is located between the Tyrrhenian and Ionian Seas, with coasts oriented from the NW–SE to NE–SW (Figure 1a). Analogously, the beach's width varies from about 80 m to 20 m. Ionian Sea beach is ENE–WSW oriented, and its width varies from about 30 m to a few meters. Due to the significative coastal erosion, this sector was protected by several breakwater groins.

In the study area of the Sicilian Tyrrhenian coast, the main direction of sea waves and storms monitored in the NW Sicilian coast over the last 1.5 years was W (270° N) and NW (285° N), respectively [58,59]. The sea bottom slope, which stretches from the shoreline to the 5 m isobath, shows inclinations of 3.6%, and marine coastal currents along the shoreline are responsible for a potential solid transport, parallel to the coast, from W to E.

In the study area of the Sicilian Ionian coast, the main direction of the low–medium waves and storms monitored in the last 14.5 years indicates a provenance from the E (90° N), with wave heights of about 6 m [58,59]. The sea bottom slope, which stretches from the shoreline to the 5 m isobath, shows inclinations of 2.8%, and marine coastal currents along the shoreline are responsible for a potential solid transport parallel to the coast, mostly from the SSW to NNE [58,59], but opposite transport directions have also been identified near the shore.

Tide currents in the northern edge of the strait move ENE and WSW during the ascending and descending phases, respectively.

In these wave-dominated beaches, significant marine shoreline migration affected the study area, including Cape Peloro. Coastline changes may depend on several local- and global-scale factors (sediment supply by river/stream transport, urbanization of the coasts, construction of coastal protective structures and ports, frequency and intensity of storms, and relative global sea level changes connected to climate change). The decrease in river sediment supply, mainly due to anthropogenic activities (such as the construction of river bridges and cement bottom coverage), the expansion of urbanized coasts, and the increasing frequency and intensity of sea storms, may be the leading factors, playing an important role in the erosion of the coasts and the regression of the coastline. In the study area, during the last two centuries, Tyrrhenian beaches “tend to be naturally stable within the same sector, resulting in a change in shape without any loss in volume” [60]. Notwithstanding this, in 2012, some sites underwent strong erosion, which was responsible for the loss of about 12,000 m² of beach, whereas Pylon beach underwent an accretion of about 5000 m² [60]. The wind increased in intensity since 2005 and the trends for winds coming from the WNW–NW and from the NW to the NNE increased and decreased, respectively [60].

The Cape Peloro area is characterized by high levels of biodiversity; however, this has been insufficiently investigated. For example, environmental associations placed great emphasis on sedentary and migratory avifauna, but little scientific literature is available

in this regard [61]. Most of the vegetation is not native, except for residual patches of autochthonous essences, which may even be endemic, that persist in a few dunes that are not yet totally anthropized [62,63]. The beaches do not host relevant biotic communities due to their small breadth and intense human attendance. Similarly, the intertidal zone is poorly represented due to the microtidal regime and steep slope of the shoreline.

In the coastal marine environment, some protected habitats are recognizable, such as the *Posidonia oceanica* beds, with a patch ranging from few meters to almost one kilometer off the coastline, at 2–45 m depth [64], and deeper, wider, coralligenous assemblages [65].

As far as the brackish basins are concerned, the literature containing information about Lake Ganzirri's biodiversity is limited [66]. This is different to the literature concerning the highly biodiverse Lake Faro, for which some faunal and floristic lists have been published [67,68], as well as data on different biological items (e.g., [69]). Only in the last decade a revised list of the macroalgal flora and their molecular bases has been underway [70–73]. Of particular interest is the presence of the threatened bivalve *Pinna nobilis* Linnaeus, 1758, which was originally abundant along the Strait of Messina coasts [74], before the mass mortality event that wiped out the marine populations of the Mediterranean [75], except in a few brackish basins, such as Lake Faro [76].

The study's marine beach deposits are composed of Holocene siliciclastic sands and heterometric gravels, which are delimited seawards by a peculiar belt of bedded siliciclastic conglomerates [77] that weakly plunge seawards. They are composed of polygenic deposits, with pebbles, cobbles, and boulders floating in arenites. They are very hard because they are pervasively cemented by carbonates. Conglomerates are encrusted with Serpulids, showing a calibrated Accelerator Mass Spectrometry (AMS) radiocarbon age of about 5.9 Ka [78]. Ganzirri beach rock is characterized by a mixture of benthic assemblages belonging to the upper littoral level or fringe [79]. Beach rock forms a very shallow marine platform that is several meters wide [80], localized from an elevation of 0.70 m to the isobath -2 m [78] and partially covered by sand for tens of km, from Mortelle in the Tyrrhenian coast to the port of Messina on the Ionian side. These beach rocks exert an important natural defensive action against coastal erosion because they induce the damping of wave energy on the coastal plain.

The Cape Peloro peninsula is delimited onshore by the hills forming the northern edge of the Peloritani Mountains (Figure 1a). These hills are made up of Quaternary siliciclastic deposits with seawards-plunging clinofolds (Sands and Gravels of the Messina Formation, Middle Pleistocene) that are underlying the Holocene deposits and form the sea bottom of the Cape Peloro peninsula [77,81–83]. The study area [84], as well as the Calabria–Peloritani Arc, is affected by strong active tectonics, which are responsible for the high seismic risk in the Straits of Messina [85,86].

5. Materials and Methods

A field survey was carried out onshore and offshore in the study area in order to search for ACMs. The marine backshore and foreshore areas, including the dunes in the Tyrrhenian coast and the cliffs along the Ionian Sea, were investigated. Punctual observations were carried out in the marine shoreface and offshore transition areas, where snorkeling and scuba-diving activities took place. Punctual observations were also made in the reserve, in two localities, 100 m wide, for comparative purposes.

After alerting the competent authorities about the presence of possible dangerous ACM wastes, university researchers, supported by authorized personnel, were involved in field activities, collecting samples of the presumed ACMs to ascertain their dangerous and toxic nature. The ACM samples were investigated by means of Optical Microscopy (OM), Scanning Electron Microscopy coupled with X-ray Energy-Dispersive Spectrometer (SEM-EDS), and Fourier Transform InfraRed (FTIR) spectroscopy techniques.

The OM observations were carried out to characterize the morphological and morphometric features, color, aspect, ornamentations, encrusting organisms, and size of the asbestos fibers of the presumed ACMs. The instrument used was a Zeiss, Stereo Discovery

model coupled to a telecamera and workstation. Photomicrographs of selected fibers were documented under stereomicroscope. Fibers were first collected after dissolution of the calcareous component of the cement in HCl, diluted at 10% and separated from the fiberglass. Then, fibers were placed in a drop of distilled water, which was dispersed onto a microscope glass, before the latter was given a glass cover. The OM observations were made in the laboratories of the University of Messina.

Morphometric analyses were carried out to determine the different geometric properties of the particles, describing the outer shape of the particles at the macro-, meso-, and microscales, and the surface texture [87,88]. The 3D shape of coarse grains/particles (pebbles/boulders) may be expressed by the long axis ($L = \text{long or } a$), the medium axis ($I = \text{intermediate or } b$), and the short axis ($S = \text{short or } c$). The morphology of particles may be expressed by a plethora of shape rates. The I/L ratio (elongation ratio or aspect ratio (AR)) [89,90] (Table 1) and S/I ratio (flatness ratio, Table 1) represent the most important aspects of particle shape [88]. The other two shape parameters that are widely used in sedimentology are the sphericity (Table 1) and roundness. For 2D measurements, the Riley sphericity is expressed by the square root of the diameter of the largest circle inscribed in the particle (D_i) divided by the smallest circle circumscribing the particle (D_c). Riley sphericity and elongation may be considered as different ways to describe the particle shape, based on the ratios of their length and width. The roundness consists of the curvature of the corners or the surface roughness. This may be obtained by visual comparison with particle charts or by applying some formula. The elongation and flatness ratios may also be plotted in the Zingg diagram in order to classify the shapes as bladed, oblate (or disc), equant, or prolate.

Table 1. Classes of elongation and sphericity. Source: Authors.

Elongation (I/L)	Classes	Sphericity	Classes
Not elongated	0.80–1.00	Very low	0.00–0.45
Slightly elongated	0.60–0.80	Low	0.45–0.63
Moderately elongated	0.40–0.60	Moderate	0.63–0.78
Very elongated	0.20–0.40	High	0.78–0.89
Extremely elongated	0.00–0.20	Very high	0.89–1.00

The LIS dimensions of the ACMs were measured on the field using a caliper and analysed by means of dedicated free software for morphometric analysis (Image J). For each examined shape parameter, the following statistical data were reported in the box plot: minimum value (Q0); first quartile (Q1); median value (Q2); third quartile (Q3); maximum value (Q4); standard deviation.

The SEM observations were taken to characterize the morphology and size of the fibers, as the SEM can provide micro- to nanoscale morphological information of the sample surface. X-ray microanalyses were carried out to determine the sample composition. The system used was a ThermoFisher SEM, Inspect s50 model, working at 10 kV and 1 nA of probe current and coupled to a Bruker Quantex X Flash 6q/60 EDS system.

FTIR spectroscopy was used to determine the main functional groups of the fibers. The instrument used was a Thermo Scientific spectrophotometer, iS50 ATR model. The scans were performed at a resolution of 4 cm^{-1} . According to the current environmental legislation, a few milligrams of ACM were analysed to ascertain the presence of chrysotile. The crocidolite is not usually investigated by this technique because its characteristic peaks are covered by the background signal due to the matrix components.

SEM and FTIR analyses were carried out in one of the few laboratories in Italy that is accredited for massive SEM tests on asbestos (Ambiente Lab accredia 1625, Messina, Italy) and the only one in the Messina province, registered in the Ministry of Health official list of qualified laboratories that are authorized to conduct analyses of asbestos.

As a precautionary principle, considering the presumed hazard posed by all the study materials, their morphometry and morphology were determined and documented by means of high-resolution photography (using a Nikon telecamera, Z30 Model). Each photograph, accompanied by a reference scale, was georeferenced and plotted on a GIS-based platform (Geographic Information System; free software QGIS 3.28.10).

Analytical and sampling procedures were performed according to the criteria reported in the Italian ministerial decree of 1994 [7] and all investigations were carried out by specialized analysts using proper personal protective equipment (PPE).

6. Results

Over 520 fragments of presumed ACMs were identified, carefully documented, and photographed along a linear belt of about 1 m wide and 4500 m long along the marine beaches of the study area. The fragments were georeferenced and reported in a GIS map (Figure 1b). This material was also associated with other anthropogenic inorganic wastes, such as thousands of fragments of bricks, tiles, cement, and colored glass.

Onshore, the ACMs were documented not only on the surface of the beaches (Figure 2) but also inside the beach deposits or exposed on natural cliffs due to the marine coastal erosion (Figure 3).



Figure 2. Fragments of ACM outcropping in the beaches of the study area (a–i). Fragments appear with well-rounded sub-elongate shapes and surface ornamentation (b). ACMs are partially covered by sands (a–e,g,i). (h,i) Boot prints on the sand showing the human–environmental interactions. The two fragments of ACM were trampled by humans, enhancing their fracture and the transfer of the fibers from the cement to humans and the environment. Source: Authors.

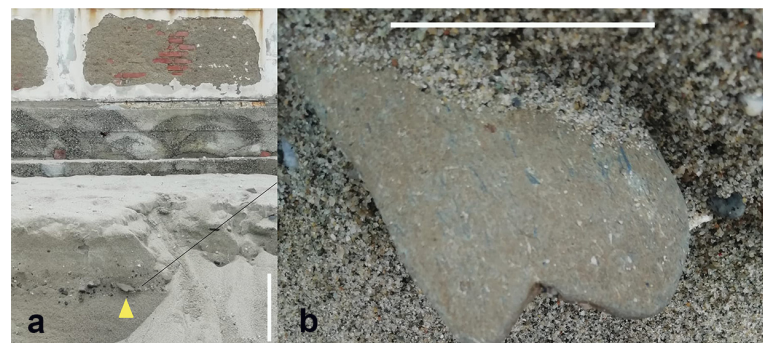


Figure 3. (a) Berm, due to marine erosion, showing beach deposits with a sandy gravel layer containing a fragment of ACM (marked by a yellow triangle). The berm is facing the entry of a building that, at present, stands about 20 m from the Tyrrhenian shoreline (Lat.: $38^{\circ}16'19.17''$ N, Long.: $15^{\circ}38'33.47''$ E). The scale bar is 0.5 m. (b) Details of Figure 3a, showing a rounded elongate shape of ACM with evidence of blue and white fibers. The scale bar is 1 m and 10 cm in Figures 3a and 3b, respectively. Source: Authors.

The removal of part of the ACMs from the beach, their transfer along the coast, and the surfacing of other ACMs were phenomena observed during the cyclic alternations of sea storms and calm sea during the winter. Evidence of sediment erosion and deposition was monitored, especially on the studied Tyrrhenian beach. The presence of berms and the exposition of old anthropogenic structures (such as wood boats, walls, and palisades contained in the beach deposits) after sea storms allowed for an estimation of erosion of at least over 1 m (Figure 4).



Figure 4. Evidence of the erosion affecting the beach of Torre Bianca facing the Tyrrhenian sea. (a) Beach near the mouth of the Canal degli Inglesi (9 January 2024) (photograph view W-wards). The

shape of the wood boat (denoted by a black line) shown in (b) is drawn for comparative purpose. (b) Erosion causes the remnants of a boat in the same area to stand out (a) (18 December 2023) (photograph view E-wards). (c) Beach in proximity to ruins and buildings (12 November 2023). (d) Same area (c) after erosion and the exposure of wood palisades (10 December 2023) (the black dog “Macchia” represents the scale). Source: Authors.

Offshore, the presence of an entire corrugated roofing sheet made of asbestos cement was ascertained at a depth of 2–3 m along the study area.

Analogous criticisms were observed in control areas located outside the O.N.R. (Figures 1a and 5).



Figure 5. Evidence of ACMs in control sites. (a,b) A decimeter size and angular fragment of ACM in a resort of the Tyrrhenian coast, neighboring the O.N.R. at Mortelle (Lat.: $38^{\circ}16'19.44''$ N, Long.: $15^{\circ}37'54.42''$ E). (c–g) Well-rounded fragments, partly broken, found on a beach along the Ionian coast, at Sant’Agata (Lat.: $38^{\circ}15'7.95''$ N, Long.: $15^{\circ}35'56.18''$ E). Source: Authors.

6.1. ACMs' Morphology and Chemical Composition

MO observations of the surfaces of the ACMs, by means of stereomicroscope, allowed for bundles of white and blue, fine, fibrous minerals (Figure 6), with a needle-like appearance, to be seen. Bundles extracted from the ACMs were also optically observed (Figure 7).

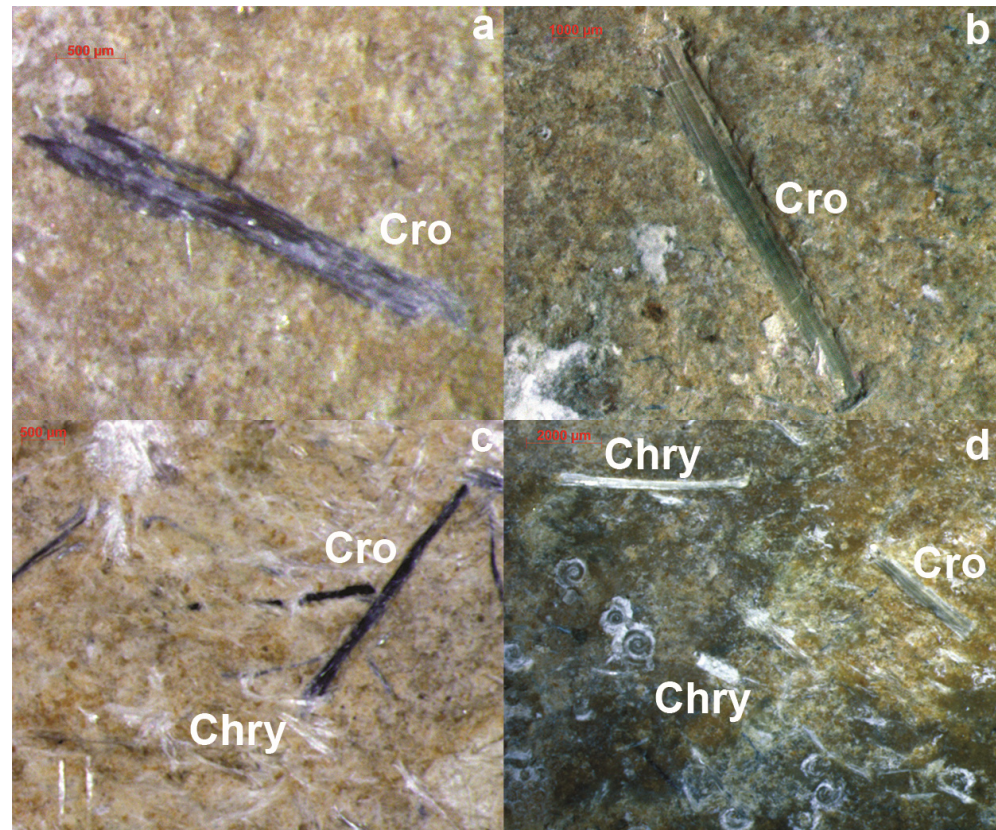


Figure 6. Microphotographs of blue and white fibrous minerals observed on the ACMs under stereomicroscope in reflected light. (a,b) Blue fibrous minerals that are compatible with asbestos-type crocidolite (Cro) according to SEM-EDS analyses. (c,d) Blue and white fibrous minerals compatible with asbestos-type crocidolite (Cro) and chrysotile according to SEM-EDS analyses. Traces of marine, calcareous, encrusting organisms (Serpulids) are presented in Figure 6d. Source: Authors.

The SEM analyses and EDS spectra of fibers of three specimens (61, 62, and 78) showed images and chemical contents compatible with asbestos-type crocidolite and chrysotile, respectively. Crocidolite fibers in the SEM images appeared light in color, with a curved morphology, whereas the EDS spectra indicated the presence of Na and high Fe contents. Analogously, chrysotile fibers appeared dark, with a straight morphology, and high and low contents, respectively, in Mg and Fe (Figure 8). The cement matrix was determined to be composed of significantly weathered carbonates.

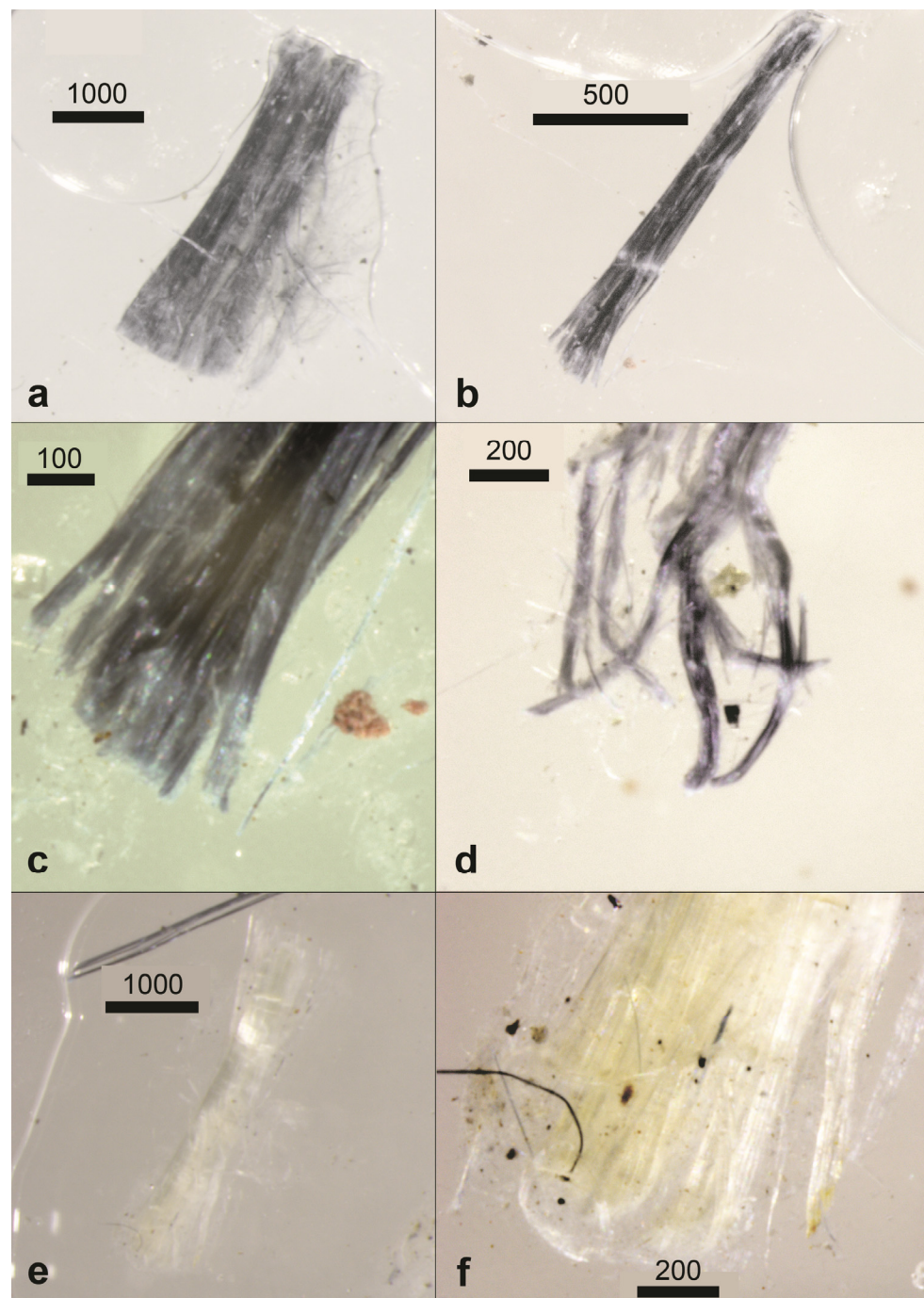


Figure 7. Photomicrographs of asbestos fibers of the studied ACMs, observed under stereomicroscope with reflected light. (a–d) Blue asbestos (crocidolite) according to SEM-EDS analyses. (e,f): White asbestos (chrysotile) according to SEM-EDS analyses. Measurement unit of scale bar is in microns. Source: Authors.

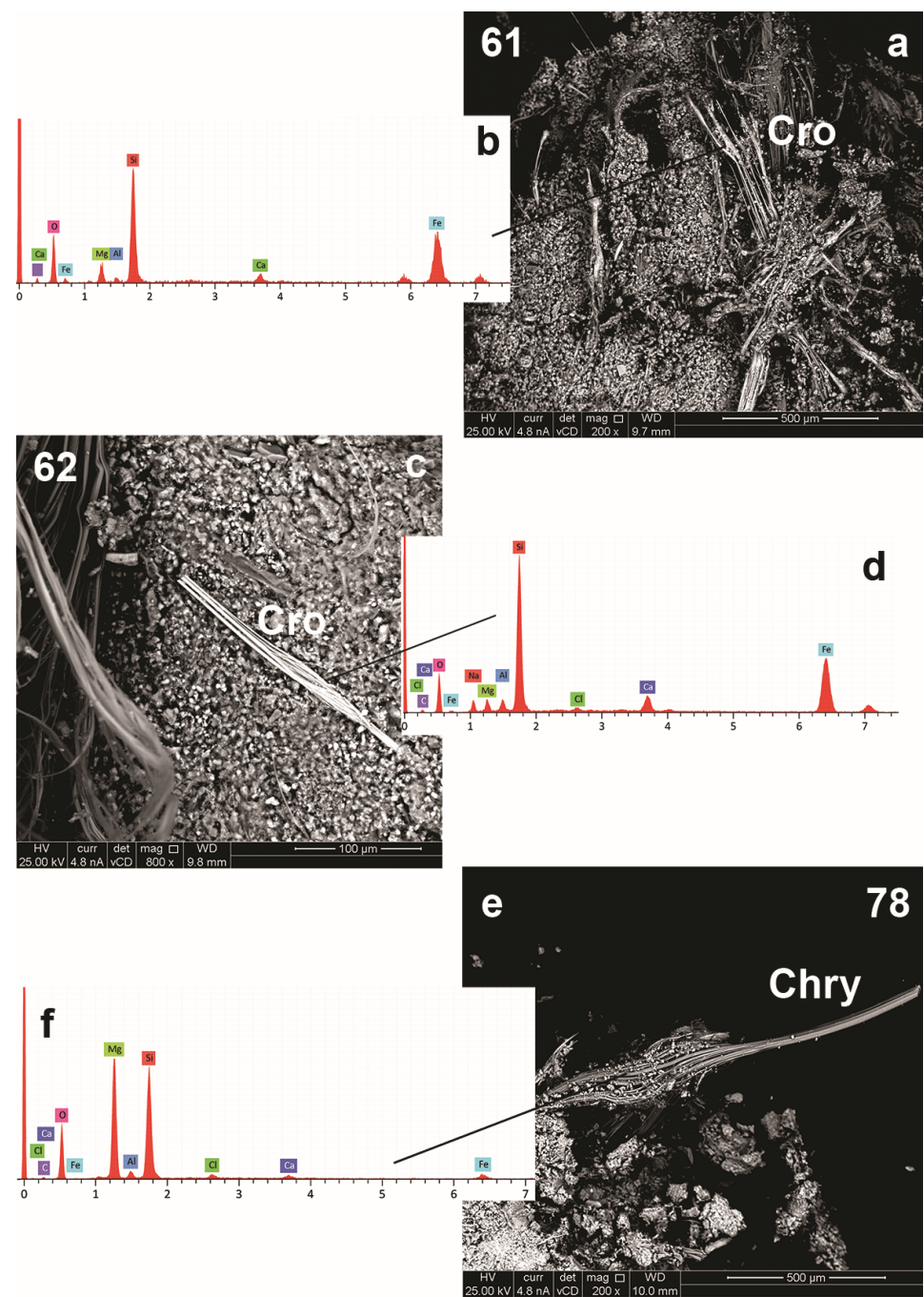


Figure 8. (a,c,e) SEM images of the asbestos fibers of specimens 61, 62, and 78. (b,d,f) EDS spectra related to specimens 61, 62, and 78.

The FTIR spectra of the asbestos fibers from the same three specimens, 61, 62, and 78, showed the inner surface Mg-OH stretch at 3644 cm^{-1} and 3686 cm^{-1} , typical of the absorbances of the chrysotile (Figure 9).

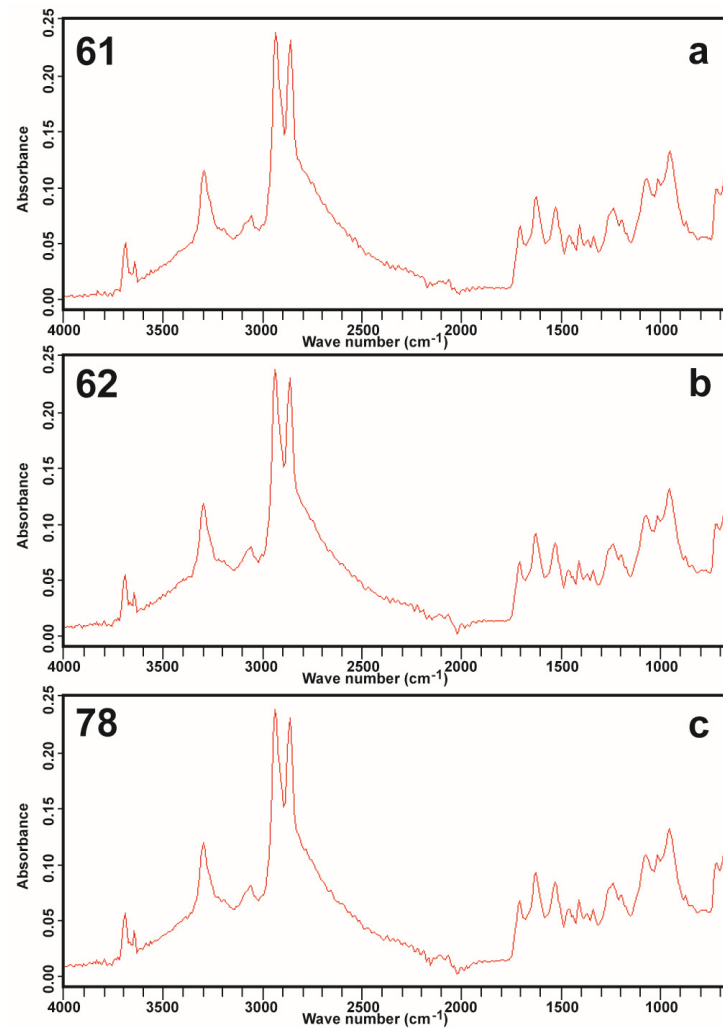


Figure 9. FTIR spectra of the asbestos fibers present in ACM specimens 61 (a), 62 (b), and 78 (c) at wave number intervals of 700–4000 cm^{-1} .

6.2. ACMs' Characteristics

Several types of ACMs were reported in the study area. These were differentiated on the basis of the following parameters and features:

- i. Color;
- ii. Face aspect;
- iii. Marine organism encrustations;
- iv. Degree of surface erosion;
- v. Shape.

The color of the ACMs' surfaces was mostly light grey, i.e., similar to the original color of the asbestos cement. A beige to orangish color (Figure 10), probably due to weathering, was also recognized in tens of fragments, especially in the Ionian beaches. Rare dark fragments and fragments of a rare dark red color were also observed (Figure 10a). This latter finding was presumably evidence of the typical red asbestos encapsulation paint usually used to protect the corrugated asbestos sheets for avoiding fiber dispersion.

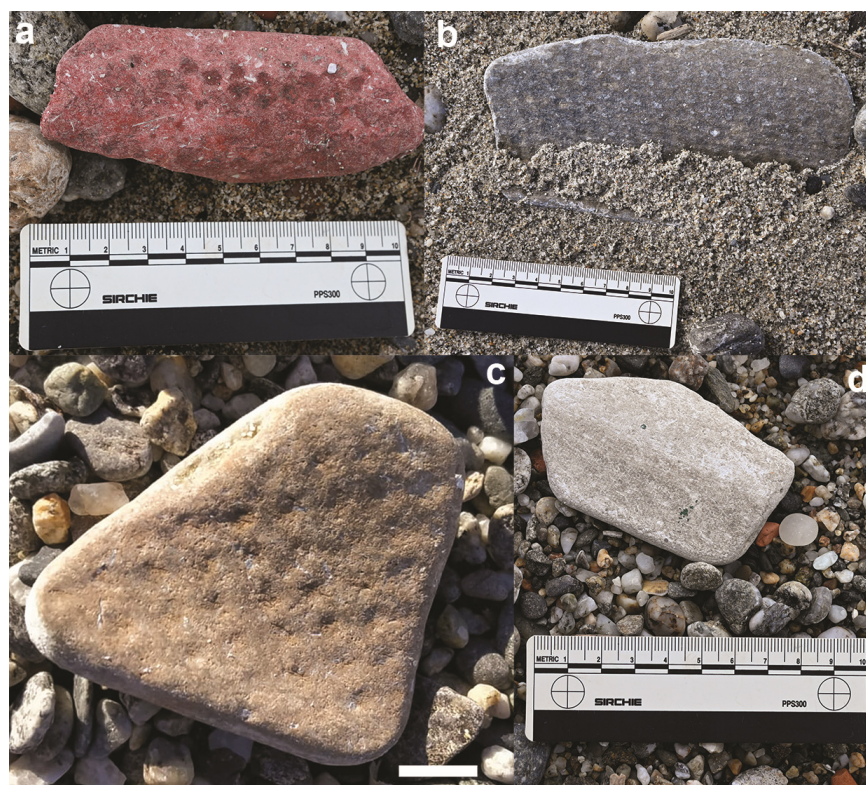


Figure 10. Colors and rough face aspect of the studied ACMs. (a) Fragment with rare dark red color of the asbestos encapsulation paint in a honeycomb-like ornamentation. (b) Fragment with typical light gray color showing honeycomb-like ornamentation. (c) Fragment with beige to orangish color showing honeycomb-like ornamentation. Scale bar: 2 cm. (d) Fragment with typical light gray color showing dome-basin like ornamentation, probably due to weathering. Source: Authors.

The face of the ACMs, mostly rough and abraded, was characterized by white and blue minerals, with the first prevailing over the second (Figure 6). Two different surface ornamentations (honeycomb-like, Figure 10a–c, and dome-basin-like, Figure 10d) were observed in tens of fragments.

MO of the surfaces of the ACMs, by means of stereomicroscope, also allowed for marine organism encrustations to be observed in a few fragments. These, present also on both sides of the ACM, were mainly formed by a complex stratification of lichens covered by calcareous red algae (*Corallinaceae*), bryozoan, and sessil gastropods (*Vermetidae*) (Figure 11).

The surface erosion of the ACMs was significant and the degree of erosion was variable from low to high. In the same fragment, homogenous or heterogenous degrees of erosion were observed. A low degree of erosion was ascertained in fragments preserving their original ornamentation and showing a thickness similar to that of the original industrial product. A high degree of erosion was evidenced by a lower thickness, the absence of ornamentation, and the erosion of the encrusted fragments (leaving some traces). Erosion/abrasion of the ACMs mostly extensively exposed the asbestos fibers on well-rounded surfaces and borders (Figure 12). Systems of incipient joints were also present. A few samples found on the beach were poorly weathered and had angular shapes and fresh fractures. However, most of the ACM angular shapes were found in materials that were abandoned on sites near the main roads.



Figure 11. (a) Field photograph and (b) microphotograph of encrusting marine organisms' growth on the surface of the ACM, observed under stereomicroscope with reflected light. Bryozoans, red algae (*Corallinaceae*), and sessile gastropods (*Vermetidae*). Scale bar: 1 cm in figure a. Source: Authors.

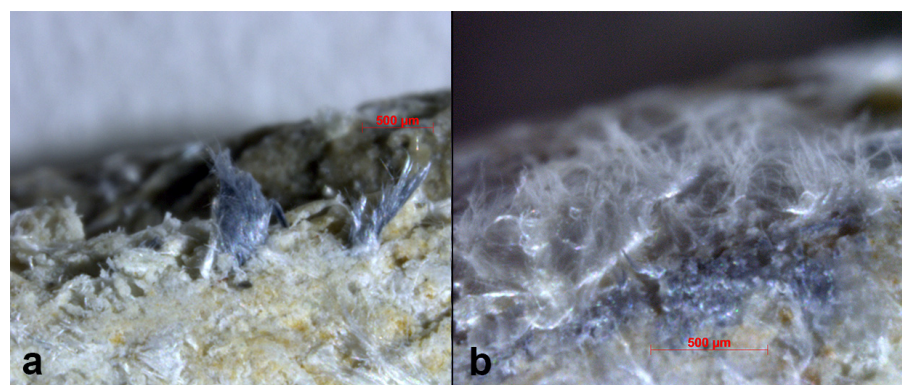


Figure 12. Photomicrographs showing the asbestos fibers exposed along the borders of the ACM's surface due to erosion/abrasion, seen under a stereomicroscope with reflected light. (a) Wisps of sub-mm long blue asbestos fibers (crocidolite). (b) Mm long white asbestos fibers (chrysotile) showing a typical wool effect. Source: Authors.

Most of the ACMs showed several cm long, well-rounded, and weathered corrugated (40–50%) and planar (50–60%) shapes, corresponding to parts of the crests and the sides of the corrugate sheets, respectively (Figure 13). Some decimeter-long specimens, showing a complete typical crest shape, were also identified (8, 28, 31, 38, 50, 54, 55, 60, 61, 62, 63, 64, 65, 66, 79 in Figure 13). Morphological and morphometric analyses were carried out to characterize the ACMs' shape (calculating elongation and flatness ratios, as well as the sphericity index and roundness).

The 3D dimensions (LIS, Figure 14) and shape parameters (F, E, R, Figure 15) were measured and calculated on 58 and 43 specimens of ACMs, respectively, and synthesized in Table 2. The LIS dimensions were found to be very heterogenous. The L and I distributions were characterized by a dextral asymmetry, whereas the S distribution was symmetric (Figure 14). The F distribution was symmetric, with the very low values typical of flatted material such as asbestos sheets (Figure 15). The E distribution was weakly right-asymmetric, with elongation values ranging from very elongated to very equant with a sub-elongated mean (Figure 15). The Riley sphericity distribution was characterized by a dextral asymmetry with values ranging from intermediate to very equant with an equant mean (Figure 15). The Zingg diagram, based on elongation and flatness ratios, showed 3D shapes shifted on the left zone of the diagram, with a very low flatness ratio and forms varying from bladed ($S < I < L$) to oblate/disc ($S < I = L$) (Figure 16).

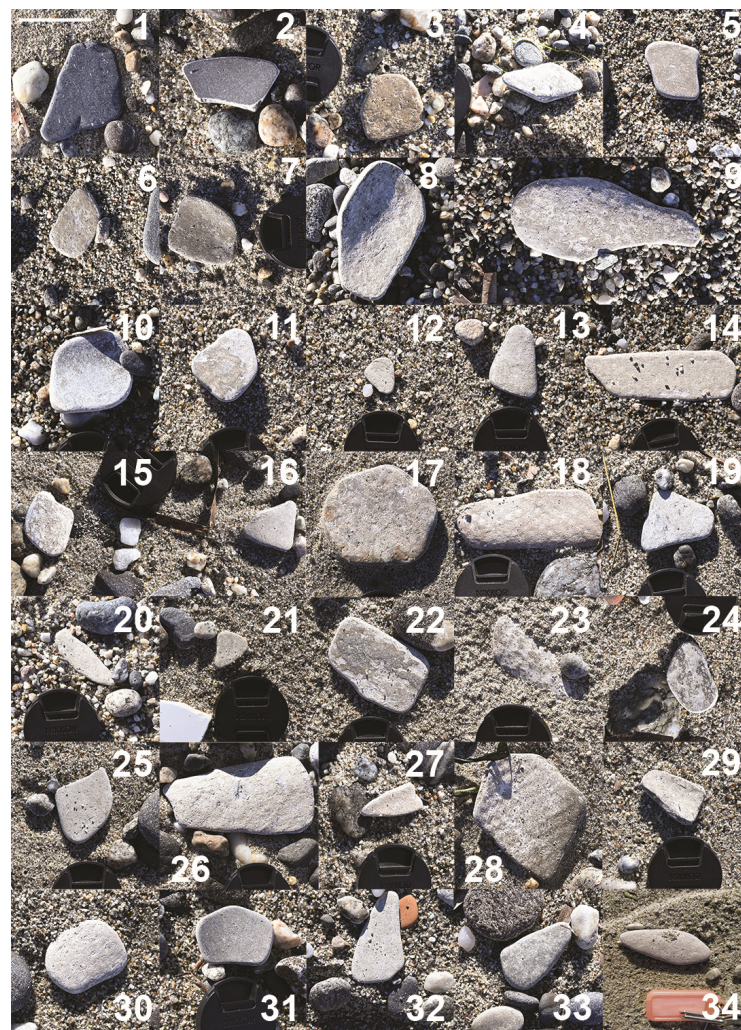


Figure 13. Cont.

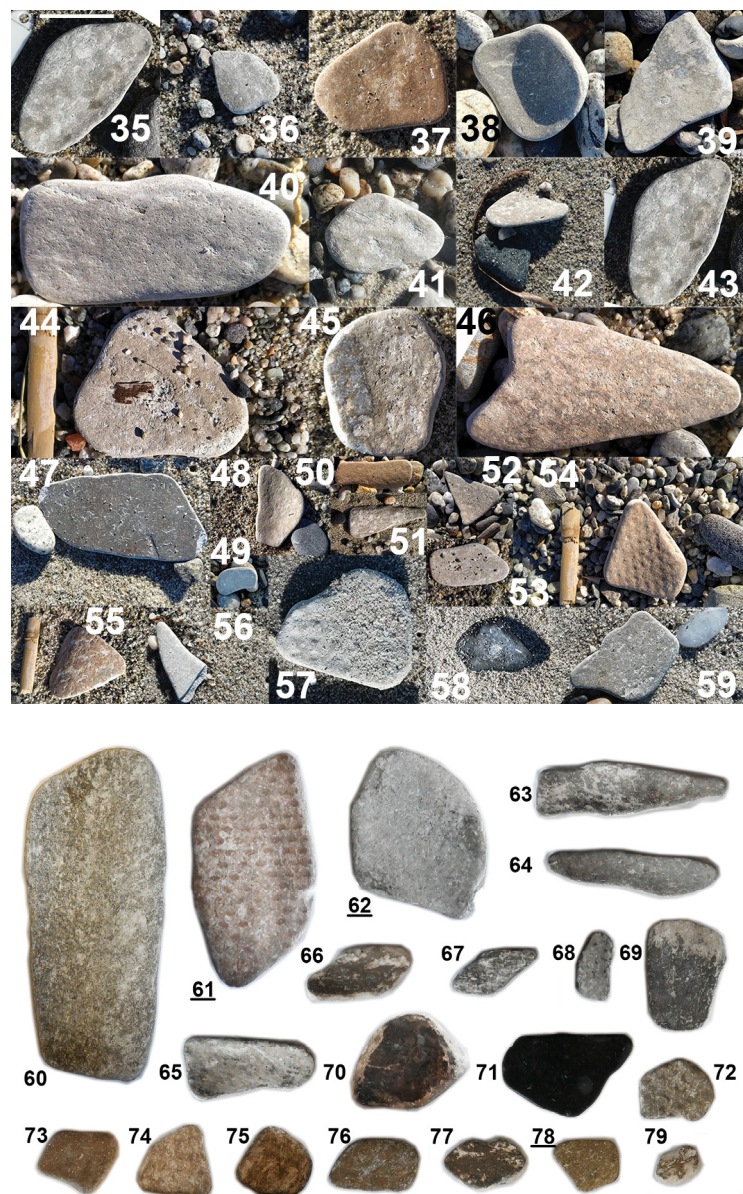


Figure 13. Representative assemblage of the main aspects and shapes of the ACMs (1–79), selected from over 520 photographs taken in the study area. Images 1–59 are related to ACMs surrounded by beach sands. To better show their aspect, images (60–79) were cut out from the sediment background using free image software. Scale bar: 5 cm. The underlined numbers indicate the samples analyzed by SEM-EDS and FTIR. Source: Authors.

Table 2. Shape parameters of the ACMs studied in the Peloro Cape. Source: Authors.

Parameter	Q ₀	Q ₁	Q ₂	Q ₃	Q ₄	St d
L (mm)	135.00	45.75	65.00	92.00	251.00	48.00
I (mm)	11.50	30.00	39.00	56.00	110.00	24.00
S (mm)	2.00	5.00	6.00	6.75	19.00	2.65
F	0.02	0.07	0.10	0.13	0.21	0.03
E	0.25	0.50	0.66	0.81	1.00	0.19
R	0.48	0.68	0.74	0.82	0.89	0.09

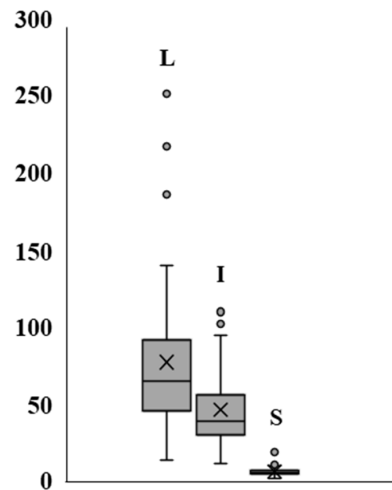


Figure 14. The 3D dimensions of the LIS orthogonal axes in the studied ACMs: L: long dimension; I: intermediate dimension; S: small dimension. The measure unit (ordinate axis) is expressed in mm. Source: Authors.

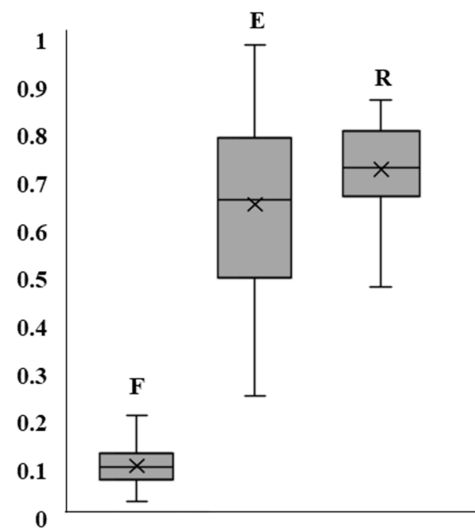


Figure 15. Shape parameters of the studied ACMs: Flatness ratio (F: S/I); elongation ratio (E: I/L); sphericity—Riley sphericity (R). Source: Authors.

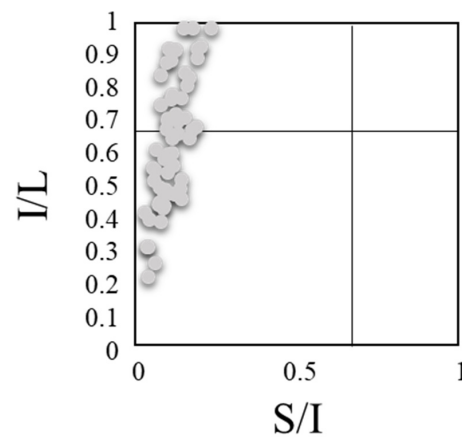


Figure 16. Zingg diagram ($S \leq I \leq L$) of the studied ACMs, showing elongation and flatness ratios in the ordinate and abscissa axes, respectively. Source: Authors.

6.3. Abandoned ACMs and Landfills

Surveys allowed for different illegally abandoned materials and landfills in the study area to be identified.

Onshore, a site showing tens cm-long, fresh, devoid of superficial vegetal growths (lichens and mosses), and angular fragments of ACMs, partially covered by brushwood, was documented in a several m² wide area (Figure 17).



Figure 17. Illegally abandoned ACMs (a–i), located behind the sand dunes exposed on the left side of the Canal degli Inglesi (Lat.: 38°16′18.96″ N, Long.: 15°38′8.98″ E). Source: Authors.

An illegal landfill of construction and building demolition wastes (mostly bricks) containing angular fragments of ACMs was located along the Ionian coast (Figure 18a–c). The presence of the landfill was evidenced by the exposure of the landfill wastes in the cliff (Figure 18a), a few meters high, facing the Ionian beach (Figure 18d–f) and eroded by the energy of the marine waves, currents, and storms. Commercial activities, parking areas, and asphalted streets actually cover the wastes.



Figure 18. Ionian coast. (a–c) Illegal landfill with fragments of ACMs (Lat.: $38^{\circ}15'37.87''$ N, Long.: $15^{\circ}37'47.19''$ E). (d–f) Beach deposits mostly comprising fragments of bricks, cement, and ACMs. The yellow arrows indicate the ACMs. Source: Authors.

7. Discussion and Conclusions

The main results of the pivotal research carried out in the protected area of Cape Peloro may be summarized as follows:

- i. The investigated material was found to be ACM containing asbestos fibers compatible with chrysotile and crocidolite (SEM-EDS and FTIR).
- ii. A high number of ACM fragments (over 520) was recorded. The ACM fragments that were found presumably represent an underestimation of the actual number dispersed in the environment.
- iii. The ACMs were observed on the top of the beach, inside beach deposits, inside illegal landfill deposits, and exposed on natural cliffs due to marine erosion. A corrugated sheet of ACM was detected on the sea bottom, at 2–3 m depth.
- iv. During winter sea storm and calm sea cycles, some of the ACMs were transported away or transferred along the coast, and other ACMs appeared on the beach.
- v. Peculiar ACM fragments were found on the beaches, covered by complex stratifications of lichens encrusted by marine calcareous red algae (*Corallinaceae*), bryozoan, and sessil gastropods (*Vermetidae*), especially in the Ionian beaches. A long period of time these colonized ACM fragments spend offshore. The age of these organisms is under study.
- vi. The most common ACM shapes found on the beach and in the beach deposits were platy with bladed and oblate forms, which were typically well rounded. The well-rounded ACM fragments are the evidence of a significative transport of these wastes. Angular shapes were also detected on the beach, and were more common in illegal landfills and abandon sites.

vii. The surface of the ACM was characterized by extensive exposure of asbestos fibers, especially in the well-rounded shapes.

The high number of ACMS fragments (11–12 fragments in each 100 m long linear area) and their unequal distribution between the Ionian and Tyrrhenian coasts (74% and 26%, respectively) agree with the respective grade of anthropization. Significantly higher concentrations, for example, were reported on the eastern side of the Due Torri canal and in some of the beaches on the strongly urbanized area of the Torre Faro coast. Analogous criticisms were reported in a few of the control areas (Annunziata, Sant'Agata, Mortelle, Figures 1a and 5).

The provenance of the ACMs and the related environmental contamination may be related to illegal landfills containing construction and building wastes and onsite abandonment, but the possibility that these wastes, which were mostly well-rounded, underwent a significative transport due to the coastal dynamics, characterized by the prevalent currents in the Tyrrhenian and Ionian Sea, cannot be discounted. Analogously, it is possible that illegal landfills and the abandonment of ACMS in streams may have significantly contributed to the anthropogenic stream sediment supply that is transferred from the Tyrrhenian and Ionian Messina valleys towards seaside areas. Significative evidence of this phenomenon is provided by the release of asbestos-bearing materials in the Ionian coastal area that occurred after the Scaletta Zanclea-Giampileri flood disaster of 1 October, 2009, and the subsequent demolition of damaged buildings [91].

Another significative issue to be considered in this case concerns the changing shoreline, which significantly affects the Tyrrhenian coast. In the western surrounding areas, especially in the Acqualadrona-Mezzana-Mulinello-Casabianca coastal area (Figure 1a), geomatic observations may show a landwards retreat of the shoreline that is estimated to range up to about 75 m in 2001–2023. It is noteworthy that, since 1969, the Tyrrhenian shoreline retreat has reached over 250 m in the most exposed coasts. On the Mezzana beach, some buildings were submerged under the sea. However, in the neighboring Tyrrhenian coast of the reserve, despite being affected by opposite land- and seawards shoreline migrations, erosion, and accretion phenomena, it may be that the ACMs found on the sea bottom could belong to previous barracks (of the fishers or farmers of "Zibibbo" vineyards) that were drowned in the sea when moving landwards.

The light weight and platy shape of the ACMs, and the strong energy of the sea storms, tides, and currents occurring in the Ionian and Tyrrhenian seas, facilitated the removal of the ACMs from local coastal illegal landfills and abandonment sites, and their transport and deposition along the coast and shallow sea. It must be underlined that the particles with original platy shapes usually remain in coastal areas because of their better adherence to the substrate. In the case of the studied ACMs, their platy shapes caused them to remain in the marine coastal and shallow environments a long time after their direct abandonment on the beach or in an ACM-bearing stream sediment supply.

The study wastes, being subject to continuous transport and wind erosion, became friable and were subject to strong abrasion due to the significant impact on their sedimentary particles. Most of the fragments showed a strong weathering of the material, with the asbestos fibers exposed on the surface of the fragments, especially along the borders. The significative degradation of the ACMs allows for the easier release of the asbestos fibers into the environment. Moreover, considering that beaches at the reserve, especially Cape Peloro, are crowded during the summer with bathers whose bodies, bath towels, and clothing are in contact with the sand, it is evident that this issue needs to be considered by the competent authorities. Consequently, an evaluation of the potential risk to both human health and the coastal marine environment should be carried out.

The marine encrustations observed on part of the ACMs, and the findings of ACM sheets at the sea bottom, suggested that a continuous transfer of this material occurs from the shallow sea to the beach and vice versa. In this regard, the evidence that the study material remains in the marine shallow environment for a long time increases the complexity of the removal activities and the consequent remediation. Consequently,

removal activities must be planned after considering a fully developed conceptual model, based on all the factors influencing the transfer mechanisms of the ACMs into the coasts and shallow marine areas.

Similar critical conditions have recently been reported in other areas of Italy [29]. Possible intervention and reclamation activities cannot limit themselves to removing the fragments on the beach, as fragments are also immersed in the coastal sediments at different depths, as well as being deposited in the sea. Any asbestos reclamation activities, if not designed and based on a multidisciplinary approach and knowledge of the local coastal dynamics and meteo-marine climate, would prove to be very expensive and ineffective, as occurred on beaches in Sardinia [41].

Italian marine beaches are maritime state property and represent an inalienable and inappropriable georesource devoted to serving the needs of the community. The ACM contamination reported in the Cape Peloro area, with a possibly detrimental impact on health, as well as elsewhere in our country, represents an issue which needs to be promptly addressed and resolved. On the basis of the above and the reports related to other Italian sites, the evidenced contamination could represent only the “tip of the iceberg”, and presumably extends much more widely. Indeed, the illegal landfill reported on the Ionian coast of the reserve could form an extensive (perhaps uneven) anthropogenic coastal plain extending landward and along the coast. Considering the widespread past use of asbestos cement in private, civil, and military buildings in the town of Messina, the present research could represent an alert sign of a “submerged criticism” affecting most of the underground areas of the metropolitan city of Messina, an overurbanized area at high seismic risk that may soon be exposed to the construction of extensive infrastructure.

Author Contributions: Conceptualization, R.S. and S.E.S.; methodology, R.S., S.G., M.M. and S.E.S.; software, R.S. and F.P.L.M.; validation, R.S., S.G., M.M. and S.E.S.; formal analysis, R.S., S.G., F.P.L.M. and M.M.; investigation, R.S., S.G. and M.M.; resources, R.S., S.G., M.M. and G.Z.; data curation, R.S., S.G. and M.M.; writing—original draft preparation, R.S.; writing—review and editing, R.S., S.G. and M.M.; visualization R.S., S.G., F.P.L.M., M.L.M., M.M., S.E.S., S.Z. and G.Z.; supervision, R.S. All authors have read and agreed to the published version of the manuscript.

Funding: This research received no external funding.

Data Availability Statement: The data is within the article.

Conflicts of Interest: The authors declare no conflicts of interest.

References

1. Directive (EU) 2023/2668 of the European Parliament and of the Council of 22 November 2023 Amending Directive 2009/148/EC on the Protection of Workers from the Risks Related to Exposure to Asbestos at Work. Available online: <https://op.europa.eu/en/publication-detail/-/publication/bacbeacf-8f22-11ee-8aa6-01aa75ed71a1/language-en> (accessed on 14 December 2023).
2. McCulloch, J.; Tweedale, G. *Defending the Indefensible. The Global Asbestos Industry and Its Fight for Survival*; Oxford University Press: Oxford, UK, 2008; pp. 1–344.
3. Silvestri, S.; Magnani, C.; Calisti, R.; Bruno, C. The experience of the Balangero chrysotile asbestos mine in Italy: Health effects among workers mining and milling asbestos and the health experience of persons living nearby. *Can Miner.* **2001**, *5*, 177–186.
4. CAS. A Division of the American Chemical Society. Available online: <https://www.cas.org/cas-data/cas-registry> (accessed on 14 December 2023).
5. Deer, W.A.; Howie, R.A.; Zussman, J. *An Introduction to the Rock-Forming Minerals*, 3rd ed.; The Mineralogical Society: London, UK, 2013; pp. 1–498.
6. Law 257/1992. Available online: https://www.salute.gov.it/resources/static/primopiano/amianto/normativa/Legge_27_marzo_1992.pdf (accessed on 15 December 2023).
7. Ministerial Decree n. of 6 September 1994. Available online: <https://www.gazzettaufficiale.it/eli/id/1994/09/20/094A5917/sg> (accessed on 16 December 2023).
8. Italian Legislative Decree n. 22 of the 5 February 1997. Available online: https://www.mase.gov.it/sites/default/files/dlgs_05_02_1997_22.pdf (accessed on 16 December 2023).

9. Directive 1999/77/EC of 26 July 1999 Adapting to Technical Progress for the Sixth Time Annex I to Council Directive 76/769/EEC on the Approximation of the Laws, Regulations and Administrative Provisions of the Member States Relating to Restrictions on the Marketing and Use of Certain Dangerous Substances and Preparations (Asbestos). Available online: <https://eur-lex.europa.eu/legal-content/EN/TXT/?uri=CELEX:31999L0077> (accessed on 16 December 2023).
10. Law 152/2006. Available online: <https://www.normattiva.it/uri-res/N2Ls?urn:nir:stato:decreto.legislativo:2006-04-03;152> (accessed on 16 December 2023).
11. Liu, Y.; Kong, F.; Santibanez Gonzalez, E.D.R. Dumping, waste management and ecological security: Evidence from England. *J. Clean. Prod.* **2017**, *167*, 1425–1437. [[CrossRef](#)]
12. Sicilian Regional Law n. 10 29 April 2014. Rules for the Protection of Health and the Territory from the Risks Deriving from Asbestos. Available online: <http://www.gurs.regione.sicilia.it/Gazzette/g14-19o/g14-19o.pdf> (accessed on 18 December 2023).
13. Paglietti, F.; Malinconico, S.; Della Staffa, B.C.; Bellagamba, S.; De Simone, P. Classification and management of asbestos-containing waste: European legislation and the Italian experience. *Waste Manag. Res.* **2016**, *50*, 130–150. [[CrossRef](#)] [[PubMed](#)]
14. Bunnell, J.E.; Finkelman, R.B.; Centeno, J.A.; Selinus, O. Medical Geology: A globally emerging discipline. *Geol. Acta* **2007**, *5*, 273–281.
15. VII Rapporto del Registro Nazionale dei Mesoteliomi (ReNaM), Italia. 2021. Available online: <https://www.inail.it/cs/internet/comunicazione/pubblicazioni/catalogo-generale/pubbl-il-registro-nazionale-mesoteliomi-settimo-rapporto.html> (accessed on 7 January 2024).
16. Kakooei, H.; Marioryad, H. Evaluation of exposure to the airborne asbestos in an automobile brake and clutch manufacturing industry in Iran. *J. Pharmacol. Toxicol.* **2010**, *56*, 143–147. [[CrossRef](#)] [[PubMed](#)]
17. Ramos-Bonilla, J.P.; Cely-García, M.F.; Giraldo, M.; Comba, P.; Terracini, B.; Pasetto, R.; Silva, Y.A. An asbestos contaminated town in the vicinity of an asbestos-cement facility: The case study of Sibaté, Colombia. *Environ. Res. J.* **2019**, *176*, 108464. [[CrossRef](#)] [[PubMed](#)]
18. Platek, S.F.; Riley, R.D.; Simon, S.D. The classification of asbestos fibres by scanning electron microscopy and computer-digitizing tablet. *Ann. Occup. Hyg.* **1992**, *36*, 155–171. [[CrossRef](#)] [[PubMed](#)]
19. Huuskonen, O.; Kivisaari, L.; Zitting, A.; Taskinen, K.; Tossavainen, A.; Vehmas, T. High-resolution computed tomography classification of lung fibrosis for patients with asbestos-related disease. *Scand. J. Work Environ. Health* **2001**, *27*, 106–112. [[CrossRef](#)] [[PubMed](#)]
20. Serio, G.; Vimercati, L.; Pennella, A.; Gentile, M.; Cavone, D.; Buonadonna, A.L.; Scattone, A.; Fortarezza, F.; De Palma, A.; Marzullo, A. Genomic changes of chromosomes 8p23.1 and 1q21: Novel mutations in malignant mesothelioma. *Lung Cancer* **2018**, *126*, 106–111. [[CrossRef](#)]
21. Klebe, S.; Leigh, J.; Henderson, D.W.; Nurminen, M. Asbestos, smoking and lung cancer: An update. *Int. J. Environ. Res. Public Health* **2020**, *17*, 258. [[CrossRef](#)]
22. Hocking, A.J.; Thomas, E.M.; Prabhakaran, S.; Jolley, A.; Woods, S.L.; Soeberg, M.J.; Klebe, S. Molecular Characterization of Testicular Mesothelioma and the Role of Asbestos as a Causative Factor. *Arch. Pathol. Lab. Med.* **2023**, *147*, 1446–1450. [[CrossRef](#)] [[PubMed](#)]
23. Wagner, J.C. The discovery of the association between blue asbestos and mesotheliomas and the aftermath. *J. Occup. Environ. Med.* **1991**, *48*, 399–403. [[CrossRef](#)] [[PubMed](#)]
24. Attanoos, R.L.; Churg, A.; Galateau-Salle, F.; Gibbs, A.R.; Roggli, V.L. Malignant mesothelioma and its non-asbestos causes. *Arch. Pathol. Lab. Med.* **2018**, *142*, 753–760. [[CrossRef](#)] [[PubMed](#)]
25. Kindler, H.L. Peritoneal mesothelioma: The site of origin matters. *Am. Soc. Clin. Oncol. Educ. Book* **2013**, *33*, 182–188. [[CrossRef](#)] [[PubMed](#)]
26. Zhai, Z.; Ruan, J.; Zheng, Y.; Xiang, D.; Li, N.; Hu, J.; Dai, Z. Assessment of global trends in the diagnosis of mesothelioma from 1990 to 2017. *JAMA Netw. Open* **2021**, *4*, e2120360. [[CrossRef](#)] [[PubMed](#)]
27. Walker-Bone, K.; Benke, G.; MacFarlane, E.; Klebe, S.; Takahashi, K.; Brims, F.; Sim, M.R.; Driscoll, T.R. Incidence and mortality from malignant mesothelioma 1982–2020 and relationship with asbestos exposure: The Australian Mesothelioma Registry. *Occup. Environ. Med.* **2023**, *80*, 186–191. [[CrossRef](#)] [[PubMed](#)]
28. Ambrose, K.K.; Box, C.; Boxall, J.; Brooks, A.; Eriksen, M.; Fabres, J.; Fylakis, G.; Walker, T.R. Spatial trends and drivers of marine debris accumulation on shorelines in South Eleuthera, the Bahamas using citizen science. *Mar. Pollut. Bull.* **2019**, *142*, 145–154. [[CrossRef](#)]
29. Lisco, S.; Lapietra, I.; Laviano, R.; Mastronuzzi, G.; Fracchiolla, T.; Moretti, M. Sedimentological features of asbestos cement fragments in coastal environments (Taranto, southern Italy). *Mar. Pollut. Bull.* **2023**, *187*, 114469. [[CrossRef](#)]
30. Tolosa, I.; Readman, J.W.; Fowler, S.W.; Villeneuve, J.P.; Dachs, J.; Bayona, J.M.; Albaiges, J. PCBs in the western Mediterranean. Temporal trends and mass balance assessment. *Deep Sea Res. Part II Top. Deep. Sea Res. Part II Top. Stud. Oceanogr.* **1997**, *44*, 907–928. [[CrossRef](#)]
31. El Nemr, A.; El-Sadaawy, M.M. Polychlorinated biphenyl and organochlorine pesticide residues in surface sediments from the Mediterranean Sea (Egypt). *Int. J. Sediment Res.* **2016**, *31*, 44–52. [[CrossRef](#)]
32. Ragab, S.; El Sikaily, A.; El Nemr, A. Concentrations and sources of pesticides and PCBs in surficial sediments of the Red Sea coast, Egypt. *Egypt J. Aquat. Res.* **2016**, *42*, 365–374. [[CrossRef](#)]

33. Reinold, S.; Herrera, A.; Hernández-González, C.; Gómez, M. Plastic pollution on eight beaches of Tenerife (Canary Islands, Spain): An annual study. *Mar. Pollut. Bull.* **2020**, *151*, 110847. [CrossRef] [PubMed]
34. Noor, T.; Javid, A.; Hussain, A.; Bukhari, S.M.; Ali, W.; Muhammad Akmal, M.; Hussain, S.M. Types, sources and management of urban wastes. In *Urban Ecology*; Verma, P., Singh, P., Singh, R., Raghubanshi, A.S., Eds.; Elsevier: Issy-les-Moulineaux, France, 2020; pp. 239–263.
35. Legambiente. Available online: <https://www.legambiente.it/rapporti-e-osservatori/liberi-dallamianto/> (accessed on 2 December 2023).
36. Osservatorio Nazionale Amianto (ONA). Available online: <https://onatotiziarioamianto.it/amianto-spiagge-necessario-effettuare-bonifica/> (accessed on 2 December 2023).
37. Il Secolo XIX. Available online: <https://www.ilsecoloxix.it/imperia/2013/05/09/news/amianto-emergenza-in-spiaggia-1.32312548> (accessed on 2 December 2023).
38. Gruppo d'Intervento Giuridico (GrIG). Associazione Ecologista. Available online: <https://gruppodinterventogiuridicoweb.com/2022/05/15/cagliari-bonificata-dai-detriti-di-amianto-la-spiaggia-del-poetto/> (accessed on 2 December 2023).
39. La Nuova di Venezia e Mestre. Available online: <https://nuovavenezia.gelocal.it/venezia/cronaca/2010/01/21/news/venezia-quintali-di-eternit-nella-cittadella-del-cinema-1.1337278> (accessed on 3 December 2023).
40. GalluraOggi.it. Available online: <https://www.galluraoggi.it/cronaca/eternit-marina-maria-bonifiche-spiaggia-2-aprile-2023/> (accessed on 3 December 2023).
41. LinkOristano.it. Available online: <https://www.linkoristano.it/2020/06/11/bene-la-pulizia-della-spiaggia-ad-abarossa-ce-ancora-amianto/> (accessed on 3 December 2023).
42. RomaToday.it. Available online: <https://www.romatoday.it/cronaca/amianto-via-del-pesce-luna-fiumicino.html> (accessed on 3 December 2023).
43. FondiNotizie.net. Available online: https://www.fondinotizie.net/notizie/territorio/52/una-spiaggia-fatta-di-amianto#google_vignette (accessed on 3 December 2023).
44. La Nazione. Available online: <https://www.lanazione.it/viareggio/cronaca/eternit-spiaggia-libera-c9217e92> (accessed on 5 December 2023).
45. Il Tirreno. Available online: <https://www.iltirreno.it/piombino/cronaca/2018/04/23/news/eternit-sulla-spiaggia-della-sterpaia-1.16748868> (accessed on 5 December 2023).
46. LaRegione. Available online: <https://www.laregione.ch/estero/estero/1602113/lastre-eternit-lucca-viareggio-ambiente> (accessed on 5 December 2023).
47. QuiCosenza.it. Available online: <https://www.quicosenza.it/news/provincia/42898-ancora-amianto-sul-litorale-di-san-lucido-spiagge-sotto-sequestro> (accessed on 5 December 2023).
48. BrindisiReport.it. Available online: <https://www.brindisireport.it/cronaca/frammenti-di-Eternit-abbandonati-da-anni-su-spiaggia-di-Specchiolla.html> (accessed on 5 December 2023).
49. OsservatorioOggi.it. Available online: <http://www.osservatoriooggi.it/notizie/attualita/5694-amianto-torre-cane-spiaggia-bambini-turisti-fasano> (accessed on 15 February 2024).
50. Ilnuovoamico.it. Available online: <https://www.ilnuovoamico.it/2018/07/amianto-pericolo-a-ridosso-della-spiaggia-di-pesaro/> (accessed on 15 February 2024).
51. Livesicilia.it. Available online: <https://livesicilia.it/amianto-seppellito-sotto-la-sabbia-bonifica-alla-spiaggia-numero-3/> (accessed on 15 February 2024).
52. Normanno.com. Available online: <https://normanno.com/attualita/lastre-amianto-due-passi-dal-mare-biancuzzo-vanno-rimosse-subito/> (accessed on 15 February 2024).
53. Tempostretto.it. Available online: <https://www.tempostretto.it/news/inquinamento-sabbia-eternit-tanto-mare-sant-agata-mortelle.html> (accessed on 15 February 2024).
54. Messinatoday.it. Available online: <https://www.messinatoday.it/cronaca/indagini-spiaggia-mili-marina-rifiuti-amianto-.html> (accessed on 15 February 2024).
55. Regione Sicilia. Available online: <https://www.regione.sicilia.it/sites/default/files/2024-01/Format%20ITA030042-%20Monti%20Peloritani,%20Dorsale%20Curcuraci,%20Antennamare%20e%20area%20marina%20dello%20stretto%20di%20Messina.pdf> (accessed on 15 February 2024).
56. Regione Sicilia. Available online: <https://www.regione.sicilia.it/sites/default/files/2024-01/Format%20ITA030008%20-%20Capo%20Peloro%20-%20Laghi%20di%20Ganzirri.pdf> (accessed on 15 February 2024).
57. Ferrarini, A.; Celada, C.; Gustin, M. Preserving the Mediterranean bird flyways: Assessment and prioritization of 38 main wetlands under human and climate threats in Sardinia and Sicily (Italy). *Sci. Total Environ.* **2021**, *751*, 141556. [CrossRef]
58. Ispra Ambiente. Available online: https://www.isprambiente.gov.it/files/pubblicazioni/statoambiente/tematiche2011/05_%20Mare_e_ambiente_costiero_2011.pdf (accessed on 15 February 2024).
59. Ispra Ambiente. Available online: <https://www.isprambiente.gov.it/it/servizi/stato-delle-coste/atlante-delle-coste> (accessed on 15 February 2024).
60. Randazzo, G.; Cigala, C.; Crupi, A.; Lanza, S. The natural causes of shoreline evolution of Capo Peloro, the northernmost point of Sicily (Italy). *J. Coast. Res.* **2014**, *70*, 199–204. [CrossRef]

61. Ferrarini, A.; Celada, C.; Gustin, M. Anthropogenic Pressure and Climate Change Could Severely Hamper the Avian Metacom-
munity of the Sicilian Wetlands. *Diversity* **2022**, *14*, 696. [[CrossRef](#)]
62. Marcenò, C.; Romano, S. La vegetazione psammofila della Sicilia settentrionale. *Inf. Bot. Ital.* **2010**, *42*, 91–98.
63. Roma-Marzio, F.; Liguori, P.; Meneguzzo, E.; Banfi, E.; Busnardo, G.; Galasso, G.; Kleih, M.; Lasem, B.; Wallnöfer, B.; Bolpagni, R.;
et al. Nuove segnalazioni floristiche italiane 6. Flora vascolare. *Not. Della Soc. Bot. Ital.* **2019**, *3*, 47–53.
64. Giacobbe, S.; Spanò, N.; Manganaro, A. *Le Praterie di Posidonia oceanica (L.) Delile nello Stretto di Messina: Stato delle Conoscenze e
Prospettive. Posidonia oceanica Meadows, Conservation and Experiences*; A.M.P. “Capo Rizzuto”: Crotona, Italy; Infantino, E., Ed.;
2004; pp. 57–66.
65. Di Geronimo, I.; Giacobbe, S. Cartes des biocenoses de Détroit de Messine. In: *Bionomie des peuplements benthiques des
substrats meubles et rocheaux plio-quatérnaires du Détroit de Messine. Doc. Et Trav. IGAL* **1987**, *11*, 153–169.
66. Bottari, A.; Bottari, C.; Carveni, P.; Giacobbe, S.; Spanò, N. Genesis and geomorphologic and ecological evolution of the Ganzirri
salt marsh (Messina, Italy). *Quat. Int.* **2005**, *140141*, 150–158. [[CrossRef](#)]
67. Giacobbe, S. Biodiversity loss in Sicilian transitional waters: The molluscs of Faro Lake. *Biodivers. J.* **2012**, *3*, 501–510.
68. Vitale, D.; Giacobbe, S.; Spinelli, A.; De Matteo, S.; Cervera, J.L. “Opisthobranch” (mollusks) inventory of the Faro Lake: A Sicilian
biodiversity hot spot. *Ital. J. Zool.* **2016**, *83*, 524–530. [[CrossRef](#)]
69. Furfaro, G.; Renda, W.; Nardi, G.; Giacobbe, S. Integrative taxonomy of the bubble snails (Cephalaspidea, Heterobranchia)
inhabiting a promising study area: The coastal sicilian Faro Lake (Southern Italy). *Water* **2023**, *15*, 2504. [[CrossRef](#)]
70. Manghisi, A.; Morabito, M.; Bertuccio, C.; Le Gall, L.; Couloux, A.; Cruaud, C.; Genovese, G. Is routine DNA barcoding an
efficient tool to reveal introductions of alien macroalgae? A case study of *Agardhiella subulata* (Solieriaceae, Rhodophyta) in
Cape Peloro lagoon (Sicily, Italy). *Cryptogam. Algol.* **2010**, *31*, 423–433.
71. Bertuccio, C.; Genovese, G.; Manghisi, A.; Cruaud, C.; Couloux, A.; Le Gall, L.; Morabito, M. Changes in the benthic algal flora of
Lake Ganzirri, North-Eastern Sicily (Italy). Cambiamenti della flora bentonica del Lago di Ganzirri, Sicilia nord orientale (Italia).
Nat. Rerum **2014**, *3*, 79–91.
72. Miladi, R.; Manghisi, A.; Armeli Minicante, S.; Genovese, G.; Abdelkafi, S.; Morabito, M. A DNA barcoding survey of *Ulva*
(Chlorophyta) in Tunisia and Italy reveals the presence of the overlooked alien *U. ohnoi*. *Cryptogam. Algol.* **2018**, *39*, 85–107.
[[CrossRef](#)]
73. Manghisi, A.; Miladi, R.; Minicante, S.A.; Genovese, G.; Gall, L.L.; Abdelkafi, S.; Saunders, G.W.; Morabito, M. DNA barcoding
sheds light on novel records in the Tunisian red algal flora. *Cryptogam. Algol.* **2019**, *40*, 13–34. [[CrossRef](#)]
74. Giacobbe, S.; Leonardi, M. Les fonds à Pinna du Détroit de Messine. *Doc. Et Trav. IGAL* **1987**, *11*, 253–254.
75. Cabanellas-Reboredo, M.; Vázquez-Luis, M.; Mourre, B.; Álvarez, E.; Deudero, S.; Amores, A.; Addis, P.; Ballesteros, E.; Barrajon,
A.; Coppa, S.; et al. Tracking a mass mortality outbreak of pen shell *Pinna nobilis* populations: A collaborative effort of scientists
and citizens. *Sci. Rep.* **2019**, *9*, 13355. [[CrossRef](#)]
76. Donato, G.; Lunetta, A.; Spinelli, A.; Catanese, G.; Giacobbe, S. Sanctuaries are not inviolable: Haplosporidium pinnae as
responsible for the collapse of the *Pinna nobilis* population in Lake Faro (central Mediterranean). *J. Invertebr. Pathol.* **2023**, *201*,
108014. [[CrossRef](#)]
77. Bonfiglio, L.; Violanti, D. Prima segnalazione di Tirreniano ed evoluzione pleistocenica di Capo Peloro (Sicilia nord-orientale).
Geogr. Fis. Dinam. Quat. **1983**, *6*, 3–15.
78. Antonioli, F.; Ferranti, L.; Lambeck, K.; Kershaw, S.; Verrubbi, V.; Dai Pra, G. Late Pleistocene to Holocene record of changing
uplift rates in southern Calabria and northeastern Sicily (southern Italy, Central Mediterranean Sea). *Tectonophysics* **2006**, *422*,
23–40. [[CrossRef](#)]
79. Cosentino, A.; Giacobbe, S. Mollusc assemblages of hard bottom subtidal fringe: A comparison between two coastal typologies.
Biodivers. J. **2015**, *6*, 353–364.
80. Bottari, A.; Bottari, C.; Carveni, P. Tectonic genesis of the salt marshes on the Sicilian coast of the Straits of Messina (Sicily). *Alp.
Mediterr. Quat.* **2005**, *18*, 113–122.
81. Jacobacci, A.; Malatesta, A.; Motta, S. *Piano di Studi Sullo Stretto di Messina per il Collegamento della Sicilia con la Calabria: Ricerche
Geologiche*; Regione siciliana; IRES: Palermo, Italy, 1961; pp. 1–66.
82. Selli, R. Geologia e sismotettonica dello Stretto di Messina. Convegno su: L’attraversamento dello Stretto di Messina e la sua
fattibilità. *Att. Acc. Naz. Lincei* **1978**, *43*, 119–154.
83. Lombardo, G. Stratigrafia dei depositi pleistocenici della Sicilia nord-orientale. *Att. Acc. Gioenia Sc. Nat. Catania* **1980**, *12*, 84–113.
84. Guarnieri, P.; Pirrotta, C. The response of drainage basins to the late Quaternary tectonics in the Sicilian side of the Messina Strait
(NE Sicily). *Geomorphology* **2008**, *95*, 260–273. [[CrossRef](#)]
85. Presti, D.; Billi, A.; Orecchio, B.; Totaro, C.; Faccenna, C.; Neri, G. Earthquake focal mechanisms, seismogenic stress, and
seismotectonics of the Calabrian Arc, Italy. *Tectonophysics* **2013**, *602*, 153–175. [[CrossRef](#)]
86. Neri, G.; Orecchio, B.; Presti, D.; Scolaro, S.; Totaro, C. Recent seismicity in the area of the major, 1908 Messina Straits earthquake,
south Italy. *Front. Earth Sci.* **2021**, *9*, 667501. [[CrossRef](#)]
87. Krumbein, W.C.; Pettijohn, F.J. *Manual of Sedimentary Petrography*. XIV + 549 pp., 8:0, 265 Figure New York and London 1938,
(1939). D. Appleton—Century Company. 8 6.50 (30 s). *Geol. Fören. Stockh. Förh.* **1939**, *61*, 225–227. [[CrossRef](#)]
88. Blott, S.J.; Pye, K. Particle shape: A review and new methods of characterization and classification. *Sedimentology* **2008**, *55*, 31–63.
[[CrossRef](#)]

-
89. Dapples, E.C.; Rominger, J.F. Orientation analysis of fine-grained clastic sediments: A report of progress. *J. Geol.* **1945**, *53*, 246–261. [[CrossRef](#)]
 90. Folk, R.L. *Petrology of Sedimentary Rocks*; Hemphill Publishing Company: Austin, TX, USA, 1980; pp. 1–184.
 91. Tempostretto.it. Available online: <https://www.tempostretto.it/news/cronaca-post-alluvione-cittadini-scaletta-chiedono-sicurezza-salute-dopo-demolizioni-amianto-dappertutto.html> (accessed on 16 February 2024).

Disclaimer/Publisher’s Note: The statements, opinions and data contained in all publications are solely those of the individual author(s) and contributor(s) and not of MDPI and/or the editor(s). MDPI and/or the editor(s) disclaim responsibility for any injury to people or property resulting from any ideas, methods, instructions or products referred to in the content.